

## Geometrical Dependence of Decoherence by Electronic Interactions in a GaAs/GaAlAs Square Network

M. Ferrier,<sup>1</sup> A. C. H. Rowe,<sup>2</sup> S. Guéron,<sup>1</sup> H. Bouchiat,<sup>1</sup> C. Texier,<sup>3,1</sup> and G. Montambaux<sup>1</sup>

<sup>1</sup>Laboratoire de Physique des Solides, Univ. Paris-Sud, CNRS, UMR 8502, 91405 Orsay, France

<sup>2</sup>Laboratoire de Physique de la Matière Condensée, École Polytechnique, CNRS, UMR 7643, 91128 Palaiseau, France

<sup>3</sup>Laboratoire de Physique Théorique et Modèles Statistiques, Univ. Paris-Sud, CNRS, UMR 8626, 91405 Orsay, France

(Received 26 July 2007; published 9 April 2008)

We investigate weak localization in metallic networks etched in a two-dimensional electron gas between 25 and 750 mK when electron-electron ( $e$ - $e$ ) interaction is the dominant phase breaking mechanism. We show that, at the highest temperatures, the contributions arising from trajectories that wind around the rings and trajectories that do not are governed by two different length scales. This is achieved by analyzing separately the envelope and the oscillating part of the magnetoconductance. For  $T \geq 0.3$  K we find  $L_\varphi^{\text{env}} \propto T^{-1/3}$  for the envelope and  $L_\varphi^{\text{osc}} \propto T^{-1/2}$  for the oscillations, in agreement with the prediction for a single ring [T. Ludwig and A. D. Mirlin, Phys. Rev. B **69**, 193306 (2004); C. Texier and G. Montambaux, Phys. Rev. B **72**, 115327 (2005); C. Texier, Phys. Rev. B **76**, 153312 (2007)]. This is the first experimental confirmation of the geometry dependence of decoherence due to  $e$ - $e$  interaction.

DOI: 10.1103/PhysRevLett.100.146802

PACS numbers: 73.20.Fz, 73.23.-b

In a conductor, quantum electronic interference is limited by phase breaking mechanisms and can only occur below a characteristic scale  $L_\varphi$ , the phase coherence length. Understanding  $L_\varphi$  is a fundamental issue of mesoscopic physics. For samples much longer than  $L_\varphi$ , regions of typical size  $L_\varphi$  behave independently, causing disorder averaging so that only contributions of reversed interfering electronic trajectories survive. This gives rise to a small quantum correction to the average conductance, called the weak localization (WL) correction, suppressed by a magnetic field. Thus the magnetoconductance (MC) is a powerful experimental tool to measure  $L_\varphi$ , determine its temperature ( $T$ ) dependence, and identify the scattering mechanisms responsible for decoherence. For a quasi 1D diffusive wire (of width  $W \ll L_\varphi$ ), the situation is now well understood theoretically [1] and experimentally [2]: when dephasing is dominated by electron-electron ( $e$ - $e$ ) interaction,  $L_\varphi$  is well described by the Altshuler-Aronov-Khmelnitsky (AAK) theory yielding  $L_\varphi \propto T^{-1/3}$ . For a ring threaded by a flux  $\phi$ , the WL oscillates as a function of  $\phi$  with a period  $\phi_0/2$  due to interference between trajectories encircling the ring, where  $\phi_0 = h/e$  is the flux quantum. These are the Altshuler-Aronov-Spivak (AAS) oscillations [3]. It was recently pointed out in [4,5] that decoherence due to  $e$ - $e$  interaction is geometry dependent: AAS oscillations involve a length scale  $L_\varphi$  different from the one of the AAK result for the wire.

The difference can be qualitatively understood along the following lines. The WL correction is related to the Cooperon  $\mathcal{P}(t)$  which sums the contributions of closed interfering reversed trajectories  $\mathcal{C}_t$  for a time  $t$ .  $e$ - $e$  interaction can be described as a fluctuating electromagnetic field which randomizes the phase  $\Phi[\mathcal{C}_t]$  accumulated along  $\mathcal{C}_t$ . Thus the WL correction to the conductivity can be

written as

$$\Delta\sigma = -\frac{2e^2D}{\pi} \int_0^\infty dt \mathcal{P}(t) \langle e^{i\Phi[\mathcal{C}_t]} \rangle_{V, \mathcal{C}_t}, \quad (1)$$

where the average  $\langle \cdots \rangle_{V, \mathcal{C}_t}$  is taken over the fluctuations of the electric potential  $V$  and the closed diffusive trajectories  $\mathcal{C}_t$ . In order to get a qualitative picture, it is sufficient to consider the fluctuations of the phase  $\langle \Phi^2 \rangle_{V, \mathcal{C}_t}$  related to the fluctuations of  $V$  via  $\frac{d\langle \Phi^2 \rangle_V}{dt} = \int d\tau \langle V(\tau)V(0) \rangle_V$ . The power spectrum of the potential is given by the Johnson-Nyquist theorem,  $\int_0^t \langle V(\tau)V(0) \rangle_V d\tau = 2e^2TR_t$ , for the resistance  $R_t = x(t)/(W\sigma_0)$  of a wire of length  $x(t)$ , the typical distance explored by interfering trajectories for a time scale  $t$ ;  $\sigma_0$  is the Drude conductivity and  $W$  the section of the wires. Since the scaling of  $x(t)$  with  $t$  depends on the diffusion and therefore on geometry, from  $\frac{d\langle \Phi^2 \rangle_{V, \mathcal{C}_t}}{dt} \sim \frac{e^2T}{W\sigma_0} x(t)$  we see that the decoherence depends on geometrical properties. For an infinite wire,  $x(t) \sim \sqrt{Dt}$ , so that the phase fluctuation varies as  $\langle \Phi^2 \rangle_{V, \mathcal{C}_t} \sim (t/\tau_N)^{3/2}$  [6], with Nyquist time  $\tau_N \propto T^{-2/3}$ . This well-known result of AAK yields  $L_\varphi \sim L_N = \sqrt{D\tau_N} \propto T^{-1/3}$  [1,7]. However, for a finite wire or for a ring of perimeter  $L$ , the length  $x(t)$  cannot be greater than  $L$  at large times, leading to fluctuations  $\langle \Phi^2 \rangle_{V, \mathcal{C}_t} \sim t/\tau_c$  with the new time scale  $\tau_c \propto T^{-1}$ , yielding  $L_\varphi \sim L_c = \sqrt{D\tau_c} \propto T^{-1/2}$  [4,5].

In a ring, the WL involves two kinds of trajectories: those which do not enclose the ring whose dephasing is expected to be driven by  $\tau_N$  and those which enclose the ring and necessarily explore the whole system so that their dephasing is driven by  $\tau_c$ . In the Fourier series of the conductivity, the harmonic  $n=0$  (smooth part) corresponds to trajectories which do not enclose the ring and are only affected by the penetration of the magnetic field in

the wires. Therefore we expect the  $T$  dependence of the envelope to be characterized by  $L_\varphi^{\text{env}} \propto T^{-1/3}$ , as in an infinite wire. On the other hand, for harmonics  $n \neq 0$ , trajectories causing the AAS oscillations encircle the ring at least once. As a consequence the harmonics decay for  $L_\varphi \ll L$ , defined as  $e^{-nL/L_\varphi^{\text{osc}}}$  [8], is characterized by  $L_\varphi^{\text{osc}} \propto T^{-1/2}$  [9]. Thus the envelope and the oscillations of the MC are controlled by *two* different length scales.

In this Letter, we show how these two length scales can be extracted from the MC of networks fabricated from a GaAs/AlGaAs 2D electron gas (2DEG).  $L_\varphi$  is determined independently from the harmonics content of the AAS oscillations ( $L_\varphi^{\text{osc}}$ ) and from the MC envelope ( $L_\varphi^{\text{env}}$ ) between 25 and 750 mK. The main result is that  $L_\varphi^{\text{osc}}$  follows a  $T^{-1/3}$  law up to 300 mK and a  $T^{-1/2}$  law above, whereas  $L_\varphi^{\text{env}}$  follows a  $T^{-1/3}$  law up to 750 mK. This is the first experimental evidence that in the high  $T$  regime,  $L_\varphi^{\text{env}}/L \lesssim 0.3$ , the phase coherence length follows a different power law with  $T$  for harmonics 0 and 1.

Measurements were performed on two different networks described in [10], and therein denoted sample A (with electrostatic gate) and sample C (without). They consist of  $10^6$  square loops of side  $a = 1 \mu\text{m}$  for sample A (a  $1000 \times 1000$  grid connected at two opposite corners through 100 wires) and  $a = 1.2 \mu\text{m}$  for sample C (a rectangular grid of aspect ratio 5 connected at the two narrow sides). The nominal width of the wires is  $W_0 = 0.5 \mu\text{m}$ . We have measured the MC up to 4.5 T between 25 mK and 1.3 K, using a standard lock-in technique (current of 1 nA at 30 Hz). The samples were strongly depleted at low  $T$  because of the etching step used to define the network. The intrinsic electron density of the 2DEG,  $n_e = 4.4 \times 10^{15} \text{m}^{-2}$  for sample A and  $3.8 \times 10^{15} \text{m}^{-2}$  for C, is recovered by illuminating the samples for several minutes at 4.2 K. The density was determined from Shubnikov-de Haas oscillations visible above 1 T. The carrier mobility was estimated to be  $\mu = 2.2 \text{m}^2 \text{V}^{-1} \text{s}^{-1}$ , 10 times smaller than the mobility of the original 2DEG.

A typical experimental curve is shown in Fig. 1. At low magnetic field, the MC exhibits large AAS oscillations with a period corresponding to  $\phi_0/2$  per unit cell (allowing a precise determination of  $a$ ). At 55 mK, three harmonics are visible in the Fourier spectrum of the MC (inset of Fig. 1). The oscillations are damped above 60 G, but the field dependence of the envelope, due to the penetration of the magnetic field through the wires, is still clearly visible. At high  $T$ , the AAS oscillations gradually disappear even at low field and only the positive MC remains with a smaller amplitude. The first harmonic is detectable up to 750 mK and the second up to 350 mK.

In [10] only the ratio between first and second harmonics was exploited below 350 mK, whereas the present work reports new data in a broader temperature range extending into a regime where  $L_\varphi \ll L = 4a$ . Difficulties arise due to uncertainties in some sample parameters such as the real width  $W$  of the wires or the elastic mean free path  $\ell_e$ . This

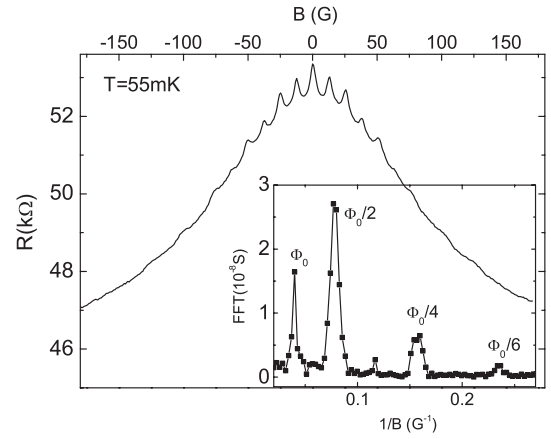


FIG. 1. Magnetoresistance of network C at 55 mK. Inset: Fast Fourier transform of the MC after subtraction of the envelope. The first peak corresponds to Aharonov-Bohm oscillations.

is why we have developed the following strategy to extract  $L_\varphi$  as a function of  $T$  (and other parameters) with the least possible parameters. At high  $T$  ( $\geq 1$  K) decoherence is dominated by electron-phonon interaction and is well described in Eq. (1) by a simple exponential  $\langle e^{i\Phi[C_i]} \rangle_{V,C_i} = e^{-t/\tau_\varphi}$  independent on trajectories, where  $\tau_\varphi = L_\varphi^2/D$ . In this case the theoretical calculation for the WL correction to the conductance of a square network [10,11]  $\Delta G = C \Delta \tilde{\sigma}(L_\varphi, \phi) = C[\Delta \tilde{\sigma}_{\text{env}}(L_\varphi) + \Delta \tilde{\sigma}_{\text{osc}}(L_\varphi, \phi)]$  perfectly describes the experimental results [11–13].  $\phi = Ba^2$  is the flux per cell and  $\Delta \tilde{\sigma} = W \Delta \sigma$  (so that  $\Delta G$  and  $\Delta \tilde{\sigma}$  do not depend explicitly on  $W$ ).  $\Delta \tilde{\sigma}_{\text{env}}$  and  $\Delta \tilde{\sigma}_{\text{osc}}$  designate the smooth and oscillating (AAS) parts, respectively.  $C$  depends on the network and its connection to contacts [from classical combination of resistances in series and in parallel we find that the classical Drude conductance is  $G_D \approx \frac{\sigma_0 W}{3.5a}$  for geometry A; therefore  $C^A \approx 1/(3.5a)$ ; for geometry C we have  $C^C \approx 1/(5a)$ ]. At low  $T$  ( $\leq 1$  K), decoherence is dominated by  $e$ - $e$  interaction and depends on the nature of trajectories. Therefore we analyze separately the envelope and oscillating part of MC. The envelope calculated with exponential relaxation interpolates between  $\Delta \tilde{\sigma}_{\text{env}} \approx -\frac{2e^2}{h} L_\varphi$  for  $L_\varphi \ll a$  and  $-\frac{2e^2}{h} \frac{a}{\pi} \ln(L_\varphi/a)$  for  $L_\varphi \gg a$  and is not expected to depend much on the precise modelization of decoherence. On the other hand it was shown [10,13] that the experimental result is perfectly fitted by the MC curve  $\Delta \tilde{\sigma}_{\text{osc}}$  with exponential relaxation. Therefore we analyze the experiment with

$$\Delta G = C_0 \Delta \tilde{\sigma}_{\text{env}}(L_\varphi^{\text{env}}) + C_1 \Delta \tilde{\sigma}_{\text{osc}}(L_\varphi^{\text{osc}}, \phi). \quad (2)$$

To compare our measurements with the theory (2) we need 5 parameters:  $L_\varphi^{\text{osc}}$ ,  $L_\varphi^{\text{env}}$ ,  $W$ ,  $C_0$ , and  $C_1$ . To begin with, we extract directly  $L_\varphi^{\text{osc}}$  (without any other adjustable parameter) below 400 mK using the ratio of the two first harmonics of the MC [10]. Using this result we determine the prefactor  $C_1$  and eventually extract  $L_\varphi^{\text{env}}$  from the amplitude of the first harmonic up to 750 mK. Then we can determine

the width of the wires from the adjustment of the damping of the oscillating part. Finally we obtain  $L_\varphi^{\text{env}}$  and  $C_0$  for the whole range of  $T$  by fitting the MC envelope with only these two parameters.

As explained in [10], we extract  $L_\varphi^{\text{osc}}$  by comparing the experimental MC harmonics  $[\Delta G_n(T)]$  to the theoretical harmonics  $\Delta\tilde{\sigma}_n(L_\varphi^{\text{osc}})$ . Experimental Fourier peaks are integrated to account for the penetration of the magnetic field in the wires. At low  $T$  ( $\approx 300$  mK), when the second harmonic  $\Delta G_2$  is clearly visible, this allows a direct determination of  $L_\varphi^{\text{osc}}$  since the harmonics ratio  $R_{12} = \frac{\Delta\tilde{\sigma}_1}{\Delta\tilde{\sigma}_2} = \frac{\Delta G_1}{\Delta G_2}$  depends only on  $L_\varphi^{\text{osc}}/a$ . It yields  $L_\varphi^{\text{osc}}(T) \propto T^{-0.34 \pm 0.02}$  (Fig. 2), in agreement with [10].

At higher temperature,  $\Delta G_2$  is suppressed and the  $T$  dependence of  $L_\varphi^{\text{osc}}(T)$  can only be extracted from  $\Delta G_1$ . This requires the knowledge of  $C_1$ , given by  $\Delta G_1(L_\varphi^{\text{osc}}) = C_1 \Delta\tilde{\sigma}_1(L_\varphi^{\text{osc}})$ . Below 300 mK, since  $L_\varphi^{\text{osc}}(T)$  and  $\Delta G_1(T)$  are determined, we plot  $\Delta G_1$  as a function of  $L_\varphi^{\text{osc}}/a$  and superimpose experimental data with theoretical calculation for  $\Delta\tilde{\sigma}_1(L_\varphi^{\text{osc}})$  between 25 and 300 mK (inset of Fig. 2). This yields  $C_1^A \approx 1/(25a)$  and  $C_1^C \approx 1/(20a)$ . This plot shows that  $C_1$  does not depend on  $L_\varphi$  and consequently on  $T$ , which validates our assumption. It is now possible to compare directly the experimental value of  $\Delta G_1(T)$  with the theoretical  $C_1 \Delta\tilde{\sigma}_1(L_\varphi^{\text{osc}})$  (inset of Fig. 2) for the whole  $T$  range where oscillations are visible and reconstruct the curve  $L_\varphi^{\text{osc}}(T)$  up to 700 mK. The result (Fig. 2) clearly

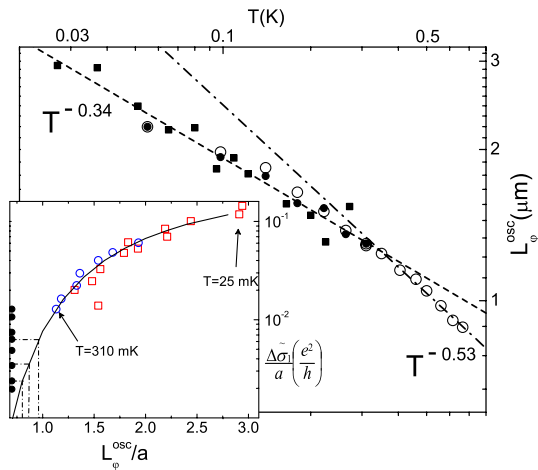


FIG. 2 (color online).  $L_\varphi^{\text{osc}}(T)$  for samples A (squares) and C (circles). Solid symbols are obtained from the ratio of the two first harmonics; open symbols are obtained with only the first harmonic. The dashed line is a fit of the low  $T$  part giving a  $T^{-0.34}$  law and the dash-dotted line is the high  $T$  fit yielding a  $T^{-0.53}$  law. Inset: continuous line is the numerical calculation of  $\Delta\tilde{\sigma}_1/a$  as a function of  $L_\varphi/a$ . Also plotted:  $\Delta G_1/(C_1 a)$  for experimental data (open squares for A and open circles for C). Solid circles on the Y axis: experimental values of  $\Delta G_1/(C_1 a)$  for sample C measured at high  $T$  when  $L_\varphi^{\text{osc}}$  is unknown. As shown on the graph  $L_\varphi^{\text{osc}}$  can be deduced from the corresponding abscissa on the theoretical curve.

shows that at high temperature  $L_\varphi^{\text{osc}}(T)$  is no longer described by the same power law. The fit of the high  $T$  data gives  $L_\varphi^{\text{osc}} \propto T^{-0.53 \pm 0.05}$ , very close to the expected  $T^{-1/2}$  for an individual ring [4,5]. It is interesting that the cross-over between the two different power laws occurs for  $L_\varphi^{\text{osc}}/a \approx 1.2$ , precisely when the second harmonic becomes unobservable. This is consistent with the fact that the network result coincides with the single ring result only when the probability for trajectories to wind around two cells is negligible [9].

Finally, the penetration of the magnetic field in the wires can be described with the substitution  $L_\varphi \rightarrow L_\varphi^{\text{eff}}(\phi)$  [14], performed for both  $L_\varphi^{\text{env}}$  and  $L_\varphi^{\text{osc}}$  [15]:

$$L_\varphi^{\text{eff}}(\phi) = L_\varphi / \sqrt{1 + \frac{1}{3} \left( 2\pi \frac{W_{\text{eff}} L_\varphi}{a^2} \frac{\phi}{\phi_0} \right)^2}. \quad (3)$$

$W_{\text{eff}} = W \sqrt{\frac{3W}{9.5\ell_e}}$  (for  $\ell_e \gg W$  and specular reflections) is the width renormalized by the phenomenon of flux cancellation [16]. This penetration causes the damping of the oscillations and the external MC envelope. First, we extract  $W_{\text{eff}}$  from the damping of the oscillations. Since at large  $\phi$   $L_\varphi^{\text{eff}}$  is independent of  $L_\varphi$ , this determination of  $W_{\text{eff}}$  is very reliable. For a given  $L_\varphi^{\text{osc}}$ , we compute the conductivity  $\Delta\tilde{\sigma}_{\text{osc}}(L_\varphi^{\text{osc}}(\phi), \phi)$ . Comparing this curve to experimental data yields  $W_{\text{eff}} = 80 \pm 5$  nm (Fig. 3). For consistency, we have checked that  $W_{\text{eff}}$  does not depend on  $T$  from 25 to 700 mK.

We then extract  $L_\varphi^{\text{env}}$  from the MC envelope by a fitting procedure. The theoretical expression of the envelope [10,11] depends only on  $W_{\text{eff}}$ ,  $L_\varphi^{\text{env}}$ , and  $C_0$ . Knowing  $W_{\text{eff}}$ , only two parameters remain, making the fit reliable. Fitting the experimental MC envelope at each  $T$  we get  $C_0^A \approx 1/(7a)$ ,  $C_0^C \approx 1/(14a)$ , and the curve  $L_\varphi^{\text{env}}(T)$  plotted in Fig. 4. The fact that  $C_0$  does not depend on  $T$  confirms the reliability of our method. The curve  $L_\varphi^{\text{env}}(T)$  yields a power law  $L_\varphi^{\text{env}} \propto T^{-0.34}$  for the whole  $T$  range.

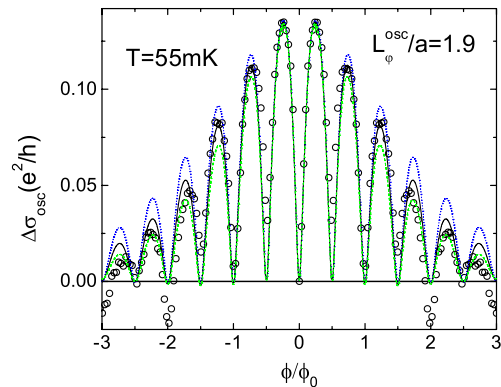


FIG. 3 (color online). Reconstruction of the damping of the oscillations after subtracting the envelope. Circles are experimental data for sample C at 55 mK. Lines correspond to theory for  $W_{\text{eff}} = 0.07a$  (dotted),  $0.08a$  (solid), and  $0.09a$  (dashed).

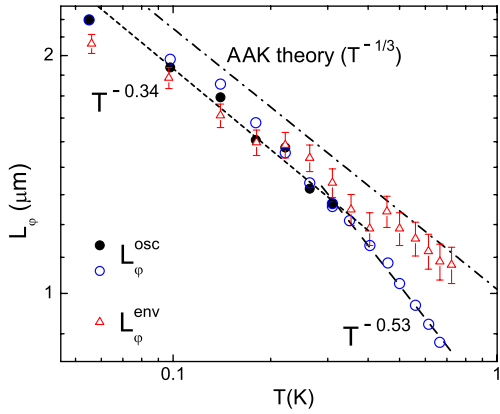


FIG. 4 (color online).  $L_\phi$  vs  $T$  for sample C. Symbols are those of Fig. 2. Empty triangles are the values extracted from the MC envelope for sample C. Dashed lines are the fit of Fig. 2 giving the power laws  $T^{-0.34}$  and  $T^{-0.53}$ . The dash-dotted line is the AAK prediction for a wire corresponding to our parameters.

From  $W_{\text{eff}}$ ,  $C_0$ , and the measurement of  $G_D = C_0 \frac{e^2}{h} k_F W \ell_e \approx 1/(46 \text{ k}\Omega)$  we obtain  $\ell_e \approx 310 \text{ nm}$  and  $W \approx 190 \text{ nm}$ , which agrees with [10]. The fact that we find  $C_0^A \approx 1/(7a)$  and  $C_0^C \approx 1/(14a)$ , instead of the expected  $C^A \approx 1/(3.5a)$  and  $C^C \approx 1/(5a)$ , shows that there probably are a significant number of broken wires [10]. This may partly explain the decoupling of the envelope and the oscillating part of the MC ( $C_0 \neq C_1$ ). However, we expect that the broken wires have little effect on the determination of  $L_\phi$  since the nontrivial shape of the MC is still very well described by the calculation of  $\Delta\tilde{\sigma}_{\text{osc}}$  that does not include this effect [17]. In the absence of a full theory for networks including the effect of  $e$ - $e$  interaction, we based our analysis on the theoretical result (2) for exponential relaxation of phase coherence instead of the single ring result [4,5]. This emphasizes nonlocal properties of quantum transport. However, we have not taken into account the fact that the pre-exponential factor of harmonics is expected to be proportional to  $L_\phi^{\text{env}}$  and not  $L_\phi^{\text{osc}}$  [5]. This may also partly explain the difference between  $C_0$  and  $C_1$ .

We now discuss the quantitative agreement of  $L_\phi^{\text{env,osc}}$  with theories. AAK [1,7] give  $L_\phi^{\text{AAK}} = \sqrt{2} \left( \frac{D^2 m^* W}{\pi k_B T} \right)^{1/3} \approx 0.88 a T^{-1/3}$ , with  $T$  in Kelvin (Fig. 4);  $m^*$  is the effective mass.  $L_\phi^{\text{env}}$  and  $L_\phi^{\text{osc}}$  are related by  $L_\phi^{\text{osc}}/a = \varpi (L_\phi^{\text{env}}/a)^{3/2}$  [4,5,8] with  $\varpi = 2^{5/4}/\pi \approx 0.75$ . We have obtained experimentally  $L_\phi^{\text{env}}/a = 0.81 T^{-1/3}$  and  $L_\phi^{\text{osc}}/a = 0.62 T^{-1/2}$  giving  $\varpi \approx 0.85$  close to theory.

In conclusion we have shown that decoherence due to  $e$ - $e$  interaction is geometry dependent. This has been revealed by demonstrating that, in the high  $T$  regime ( $L_\phi^{\text{env}}/a \lesssim 1.2$ ), the envelope of the MC and its oscillating part (AAS) are governed by different length scales  $L_\phi^{\text{env}} \propto T^{-0.34 \pm 0.02}$  and  $L_\phi^{\text{osc}} \propto T^{-0.53 \pm 0.05}$ . These  $T$  dependences are close to the expected  $L_\phi^{\text{env}} \propto T^{-1/3}$  [1] and  $L_\phi^{\text{osc}} \propto$

$T^{-1/2}$  [4,5]. Prefactors found in experiment are also consistent with theories. We emphasize that it has been possible to use the power law  $L_\phi^{\text{osc}} \propto T^{-1/2}$ , derived theoretically for a single ring, in the regime  $L_\phi^{\text{env}}/a \ll 1$  when rings of the network can be considered as independent. In the other regime  $L_\phi^{\text{env}}/a \gtrsim 1.2$ , the observed  $L_\phi^{\text{osc}} \propto T^{-0.34}$  is still unexplained [9].

We thank B. Etienne and D. Mailly for the fabrication of the heterojunctions and L. Angers, C. Bäuerle, R. Deblock, F. Mallet, A. Mirlin, L. Saminadayar, and F. Schopfer for fruitful discussions.

- [1] B.L. Altshuler, A.G. Aronov, and D.E. Khmel'nitsky, J. Phys. C **15**, 7367 (1982).
- [2] T.J. Thornton *et al.*, Phys. Rev. Lett. **56**, 1198 (1986); S. Wind *et al.*, *ibid.* **57**, 633 (1986); F. Pierre *et al.*, Phys. Rev. B **68**, 085413 (2003).
- [3] A.G. Aronov and Yu. V. Sharvin, Rev. Mod. Phys. **59**, 755 (1987).
- [4] T. Ludwig and A.D. Mirlin, Phys. Rev. B **69**, 193306 (2004).
- [5] C. Texier and G. Montambaux, Phys. Rev. B **72**, 115327 (2005); **74**, 209902(E) (2006); C. Texier, *ibid.* **76**, 153312 (2007).
- [6] G. Montambaux and E. Akkermans, Phys. Rev. Lett. **95**, 016403 (2005).
- [7] E. Akkermans and G. Montambaux, *Mesoscopic Physics of Electrons and Photons* (Cambridge University Press, Cambridge, 2007).
- [8] The result for harmonics  $\Delta\sigma_n \propto e^{-(\pi/8)n(L/L_N)^{3/2}}$  (for  $L_N \ll L$ ) [4,5] can be interpreted in two ways. (i) Scaling with  $L$  suggests  $L_\phi \rightarrow L_N \propto T^{-1/3}$ . (ii) Assuming the original AAS form  $e^{-nL/L_\phi}$  leads to a perimeter-dependent phase coherence length  $L_\phi \rightarrow L_N^{3/2}/L^{1/2} \propto T^{-1/2}$ .
- [9] Our analysis is only valid in the high  $T$  regime ( $L_\phi \ll L$ ). For  $L_\phi \gtrsim L$ , winding trajectories also explore the wires around the ring, which drastically affects the winding properties and leads to different behaviors [5].
- [10] M. Ferrier *et al.*, Phys. Rev. Lett. **93**, 246804 (2004); M. Ferrier, Ph.D. thesis, Université Paris-Sud, 2004.
- [11] B. Douçot and R. Rammal, Phys. Rev. Lett. **55**, 1148 (1985); J. Phys. (France) **47**, 973 (1986); M. Pascaud and G. Montambaux, Phys. Rev. Lett. **82**, 4512 (1999).
- [12] B. Pannetier *et al.*, Phys. Rev. Lett. **53**, 718 (1984).
- [13] F. Mallet, Ph.D. thesis, Université J. Fourier, 2006.
- [14] B.L. Altshuler and A.G. Aronov, JETP Lett. **33**, 499 (1981).
- [15] It was shown in [5] that the substitution for  $L_\phi^{\text{osc}}$  has another form for  $e$ - $e$  interaction; however, both functions are indistinguishable in practice.
- [16] H. Van Houten *et al.*, Surf. Sci. **196**, 144 (1988); Ç. Kurdak *et al.*, Phys. Rev. B **46**, 6846 (1992).
- [17] This is confirmed by the fact that a similar analysis holds for the silver networks of [13] with a negligible number of broken wires.